

Correlating Gravitational Waves with W -boson Mass, FIMP Dark Matter, and Majorana Seesaw Mechanism

Xuewen Liu, Shu-Yuan Guo, Bin Zhu*, and Ying Li†

Department of Physics, Yantai University, Yantai 264005, China

June 24, 2022

Abstract

We study a minimal extension of the Standard Model by introducing three right-handed neutrinos and a new scotogenic scalar doublet, in which the mass splittings between neutral and charged components are responsible for the W -boson mass newly measured by the CDF collaboration. This model can not only generate non-vanishing Majorana neutrino masses via the interaction of right-handed neutrinos and scotogenic scalars, but also explain the Universe's missing matter in the form of FIMP dark matter. We also study the influence of the mass splitting on the first order electroweak phase transition, and find that it can further enhance the transition strength and thus induce gravitational waves during the phase transition, which may be detected in the forthcoming detectors such as U-DECIGO.

Keywords: W boson mass, Dark matter, Neutrino, Electroweak phase transition, Gravitational waves

1 Introduction

With high precision, the Standard Model (SM) explains the interactions of all known fundamental particles. Despite of intensive investigations, no significant deviations from the SM have been identified in the experiments, suggesting that the SM constitutes the complete description of Nature. However, several long-standing issues imply that new physics beyond the SM is inevitable. The origin of neutrino masses and the formation of cold dark matter are the two primary puzzles that any extensions of the SM should address. Intriguingly, the newly measured W boson mass provides yet another impetus for new physics. Very recently, with the improved parton distribution functions of the (anti)proton and new track reconstruction, the CDF collaboration at Fermilab has released the world's most precise direct measurement of the W boson mass [1], $m_W^{\text{CDF}} = 80.4435 \pm 0.0094$ GeV, based on 8.8 fb^{-1} of data gathered between 2002 and 2011, which is approximately 7σ away from the SM prediction $m_W^{\text{EW}} = 80.3545 \pm 0.0059$ GeV [2]. Furthermore, there is a significant tension between the new CDF result and the direct measurements implemented by the D0 collaboration at the Tevatron [3] and the

*zhubin@mail.nankai.edu.cn

†liying@ytu.edu.cn

ATLAS/LHCb collaboration at the Large Hadron Collider (LHC) [4, 5] while the latter ones are in good agreement with m_W^{EW} . Although it is yet premature to confirm the existence of new physics, a number of analyses on the new data and interpretations in terms of physics beyond the SM have been carried out in the literature [6–14].

In this work, we aim to bind the three issues together and interpret them in a single setup, where we investigate the scotogenic model consisting of three right-handed neutrinos and one $SU(2)$ doublet. This matter content was first postulated in [15], which uses the scotogenic scalar as dark matter, and explains the origin of tiny neutrino masses via a loop-induced process involving the new matter contents. We found that the mass splitting between the charged and neutral components of the $SU(2)$ doublet behaves like a bridge to connect the three issues naturally. The scotogenic model is one of the simplest loop realizations of the dim-5 Weinberg operator [16]. It lowers the seesaw scale from GUT to the electroweak (EW) scale, meanwhile provides candidate for dark matter in our Universe. The presence of a scotogenic scalar also explains the latest W boson mass discrepancy. This is mainly because the authors in [7] demonstrated that the oblique parameters S , T , and U must deviate from the SM estimate to establish a consistent EW global fit, indicating the presence of mass-splitting in the scalar sector. Since the scotogenic scalar has an $SU(2)$ representation, it yields a non-vanishing contribution to oblique parameters.

The scalar sector in scotogenic model is also well known as the inert doublet model [17–21] which naturally includes a DM candidate, i.e. either the CP even Higgs or CP odd Higgs. However, the main difficulty in the original inert model is to produce the correct relic density of dark matter under the direct detection limits. Only in the Higgs funnel region (and heavy mass region), can inert scalar annihilation attain the proper relic density. On the other hand, the right-handed neutrino in this model can become a promising dark matter candidate in most parameter space. The distinctive structure of Yukawa couplings is not only helpful to achieve tiny neutrino mass but beneficial to the freeze-in production of dark matter. The Feebly Interacting Massive Particle (FIMP) couples to the thermal bath extremely weak, so that it can not retain chemical equilibrium with the thermal bath. Instead, the DM particles were produced by the decay processes from the scalar sector, which provides the correct relic abundance. In addition, the new introduced particles could also be used to explain the anomalies in flavor physics [22].

The predictability of this paradigm is an essential part of its attractiveness. Including the scotogenic scalar, the extra degrees of freedom lead to an inevitable first order electroweak phase transition (EWPT) in the early Universe. The scalar mass splittings required for explaining the W boson mass happen to affect the magnitude of phase transition. EWPT in the scotogenic scalar sector has been extensively studied [20, 21, 23, 24]. However, the new W boson mass anomaly strongly motivates us to re-study the brand new parameter space. As a consequence, the strong enough phase transitions assure the generation of gravitational waves (GWs). Astonishingly, we can use the resulting gravitational wave created to dig insight into the W bosons with the future facilities. The essential characteristics and forecasts of the scotogenic model are presented in this work.

2 Neutrino mass and dark matter

The scotogenic model [15] is one of the simplest ways to link neutrino mass to dark matter. Besides the particle content in SM, an additional doublet scalar (denoted as H_2) and three generations of right-handed neutrinos N_k ($k = 1, 2, 3$) are introduced. The new particles have odd parity under a new

Z_2 symmetry, while the SM particles are all Z_2 even. With Z_2 odd nature, the right-handed neutrinos cannot form Dirac masses $\bar{L}\tilde{H}_1N + \text{h.c.}$, where H_1 represents the SM Higgs doublet and $\tilde{H}_1 \equiv \epsilon H_1^*$. The relevant terms in the Lagrangian, concerning right-handed neutrinos, are written as

$$-\mathcal{L}_N = \frac{1}{2}m_N\bar{N}^cN + y_N\bar{L}\tilde{H}_2N + \text{h.c.} \quad (1)$$

Similar to the type-I seesaw, the right-handed neutrinos could have Majorana masses. The scalar potential, obeying SM gauge symmetries plus the discrete Z_2 , is given as

$$V = -\mu_1^2|H_1|^2 + \mu_2^2|H_2|^2 + \lambda_1|H_1|^4 + \lambda_2|H_2|^4 + \lambda_3|H_1|^2|H_2|^2 + \lambda_4|H_1^\dagger H_2|^2 + \frac{\lambda_5}{2} \left\{ (H_1^\dagger H_2)^2 + \text{h.c.} \right\}. \quad (2)$$

The conserved Z_2 parity forbids H_2 from developing a vacuum expectation value after EW symmetry breaking. However, we should mention that the existence of an additional doublet alters the EWPT, which imprints the detection signature as gravitational waves. The two doublets could be expressed as,

$$H_1 = \begin{pmatrix} \phi_1^+ \\ \frac{1}{\sqrt{2}}(v+h+i\chi) \end{pmatrix}, H_2 = \begin{pmatrix} H^+ \\ \frac{1}{\sqrt{2}}(H+iA) \end{pmatrix}, \quad (3)$$

h would be the only physical component of H_1 , and it plays the role of the observed Higgs scalar. For H_2 , the four components are all physical, with two neutral scalars, H (CP-even) and A (CP-odd), and two charged scalars, H^\pm . Generally, the quartic couplings can be written in terms of the physical scalars masses and μ_2 ,

$$\lambda_3 = \frac{2}{v^2} (m_{H^\pm}^2 - \mu_2^2), \quad (4)$$

$$\lambda_4 = \frac{(m_H^2 + m_A^2 - 2m_{H^\pm}^2)}{v^2}, \quad (5)$$

$$\lambda_5 = \frac{(m_H^2 - m_A^2)}{v^2}. \quad (6)$$

We see that the λ_5 term controls the mass difference between the two neutral components, and together with λ_4 , the mass differences in H_2 are determined. The couplings λ_i are constrained by the unitarity, vacuum stability, and perturbativity requirements (see [19] for details), and in the following analysis we have taken these constraints into account.

Now one could give a calculation on the neutrino mass in the scotogenic model, which is given by [25]

$$(\mathcal{M}_\nu)_{\alpha\beta} = \sum_{k=1}^3 \frac{y_N^{\alpha k} y_N^{\beta k}}{32\pi^2} m_{N_k} \left[\frac{m_H^2}{m_H^2 - m_{N_k}^2} \ln \left(\frac{m_H^2}{m_{N_k}^2} \right) - \frac{m_A^2}{m_A^2 - m_{N_k}^2} \ln \left(\frac{m_A^2}{m_{N_k}^2} \right) \right], \quad (7)$$

here α, β label the neutrino flavor indices. Thus the mass difference between H and A plays an important role to produce the loop neutrino mass, under the degenerate limit, i.e. $m_H = m_A$ (or $\lambda_5 = 0$), the loop mass would be vanished. If $\lambda_5 \ll 1$, the mass matrix could be rewritten as

$$(\mathcal{M}_\nu)_{\alpha\beta} = \frac{\lambda_5 v^2}{32\pi^2} \sum_{k=1}^3 y_N^{\alpha k} y_N^{\beta k} \frac{m_{N_k}}{m_0^2 - m_{N_k}^2} \times \left[1 - \frac{m_{N_k}^2}{m_0^2 - m_{N_k}^2} \ln \left(\frac{m_0^2}{m_{N_k}^2} \right) \right], \quad (8)$$

with $m_0^2 = (m_H^2 + m_A^2)/2$. The EW scale realization of neutrino mass at the present energy frontier is relevant to the low-energy experiment. Hence we focus on the masses of particles in loop below TeV. Apart from that, we would pay our attention to thermal freeze-in production of the dark matter, which

is the lightest right-handed neutrino N_1 . The out-of-equilibrium accumulation, which we discuss in the dark matter section, requires relevant coupling $y_N^{\alpha 1}$ to be extremely small. Hence N_1 contribution to neutrino mass is negligible. Such a scenario is still consistent with the neutrino oscillation result, since the converting probabilities care for the squared mass differences of neutrinos, while one vanished neutrino mass is allowed. One could estimate that to realize the neutrino mass at the TeV scale, a combining constraint is $\lambda_5(y_N^{\alpha 2,3})^2 \sim 10^{-11}$ [25]. It could be reached by tiny λ_5 while large $y_N^{\alpha 2,3}$. But actually a too large Yukawa, e.g. $y_N > 0.1$, would result in strong contradiction with the non-observation of lepton flavor violation(LFV) decays, e.g. $\ell_i \rightarrow \ell_j \gamma$.

The signature searching on collider of the new particles depends on relative sizes of their masses. If the charged scalar is the next-to-lightest Z_2 odd particle, it has no choice but to decay into N_1 , leaving a highly ionizing charged track in the detector. The null result of searching for such kind of track from heavy stable charged particle, on LHC, could exclude m_{H^\pm} up to ~ 500 GeV for $m_{N_1} \geq 1$ MeV. If the next-to-lightest Z_2 odd particle is N_2 , the searching signature would be two prompt charged leptons plus missing energy, which is from the decay of $H^\pm \rightarrow N_2 \ell^\pm$. The small decay rate of $N_2 \rightarrow \ell \bar{\ell} N_1$ would result in a decay-length which largely exceeds size of the detector. Searching for two prompt leptons plus missing energy on LHC could exclude m_{H^\pm} up to ~ 160 GeV, when assuming the prompt charged leptons are either e^\pm or μ^\pm . The exclusion limit would become weaker when decay into tau lepton is allowed. If N_3 is lighter than the charged scalar, the decay of $H^\pm \rightarrow N_3 \ell^\pm$ would open and N_3 could subsequently decay into $\ell \bar{\ell} N_2$. The relevant Yukawa couplings are strongly constrained by the non-observation of $\mu \rightarrow e \gamma$, hence may result in a signature of displaced lepton pair. The null result on LHC of the displaced lepton pair could set constraints on masses of $N_{2,3}$ and H^\pm , depends on the magnitude of Yukawa couplings. Decay products of the neutral scalars are similar to the charged one except that charged leptons are replaced by neutrinos, hence the limits on $m_{H/A}$ are weaker than the charged one. As we focus on the case that charged scalar is the lightest Z_2 odd scalar, adopting the above constraints for H^\pm are enough for the scalar sector. For detailed discussion of the collider searching, one is referred to [26]. In the following discussions, we will adopt the corresponding constraints on masses whenever the mass spectra are fixed. Besides, requirements on neutrino mass and obeying LFV decays constraints are also imposed.

The discrete Z_2 parity on one hand gives loop masses for neutrinos, on the other hand, it also suggests a candidate particle for dark matter. In principle, both the lightest neutral scalar and sterile neutrino can be dark matter. For the former situation, the neutral scalar could be thermally freeze-out produced and becomes a typical WIMP. However, due to the current stringent limits from the direct detection and relic density, most of the parameter space has been ruled out of the WIMPs [24]. Another possibility is that the lightest right-handed neutrino, i.e. N_1 , acts as a FIMP dark matter. In this situation, dark matter N_1 is produced out of thermal equilibrium. Specifically speaking, N_1 is accumulated from the decay of $X(H, A, H^\pm) \rightarrow N_1 L$, which relates to Yukawa $y_N^{\alpha 1}$ (y_1 for short thereafter). The out of equilibrium condition requires the decay rate to be smaller than the rate of Universe expansion, i.e. $\Gamma(X \rightarrow N_1 L) < H(T \sim m_X)$, which would force y_1 to be small. The dark matter N_1 yield, $Y_{N_1}(T) = n_{N_1}(T)/s(T)$, can be computed by solving the following Boltzmann equation [27]

$$sT \frac{dY_{N_1}}{dT} = -\frac{\gamma_{N_1}(T)}{H(T)}, \quad (9)$$

with $\gamma_{N_1}(T)$ representing the thermal averaged FIMP production rate

$$\gamma_{N_1}(T) = \sum_X \frac{g_X m_X^2 T}{2\pi^2} K_1(m_X/T) \Gamma(X \rightarrow N_1 \ell), \quad (10)$$

g_X is the internal degrees of freedom of X , s is the entropy density of the Universe, $H(T)$ is the expansion rate of the Universe at a given temperature and $K_1(x)$ is the Bessel function of the second kind.

The relevant study can be found in Ref. [25]. N_1 production will be dominated by the decays of the scalars (H, A, H^\pm) while they are in equilibrium with the thermal bath. The accumulation of N_1 could, in principle, also from decay of heavier sterile neutrinos, i.e. $N_{2,3} \rightarrow N_1 \bar{\ell} \ell$, but Ref. [25] has verified these decays are subdominate.

The decay rates that enter into $\Gamma(X \rightarrow N_1 L)$ are calculated as,

$$\Gamma(H \rightarrow N_1 \bar{\nu}) = \frac{(m_H^2 - m_{N_1}^2)^2}{32\pi m_H^3} y_1^2, \quad (11)$$

$$\Gamma(A \rightarrow N_1 \bar{\nu}) = \frac{(m_A^2 - m_{N_1}^2)^2}{32\pi m_A^3} y_1^2, \quad (12)$$

$$\Gamma(H^+ \rightarrow N_1 \bar{\ell}) = \frac{(m_{H^+}^2 - m_{N_1}^2)^2}{32\pi m_{H^+}^3} y_1^2. \quad (13)$$

By simply numerical calculations we can obtain the observed DM relic density with the Yukawa coupling in the range $y_1 \in [10^{-12}, 10^{-11}]$, for tens to hundreds GeV FIMPs. To study the correlations with the new CDF measured m_W and EWPT, we take $m_{H^\pm} = 300$ GeV, $y_1 = 1.48 \times 10^{-12}$ and $m_{N_1} = 100$ GeV as a benchmark. Then we find the viable parameter space for generating the relic density $\Omega h^2 = 0.12 \pm 0.0012$ [28, 29], which is shown by the purple band on mass splittings plane, see Fig. 1.

3 W boson mass and Gravitational Waves

The relationship between W boson mass and the oblique corrections is given by [30],

$$m_W^2 = m_W^2(\text{SM}) + \frac{\alpha c^2}{c^2 - s^2} m_Z^2 \left[-\frac{1}{2} \Delta S + c^2 \Delta T + \frac{c^2 - s^2}{4s^2} \Delta U \right], \quad (14)$$

where $c = \cos \theta_W$, $s = \sin \theta_W$. To generate suitable W boson mass, we resort to a significant contribution from ΔS and ΔT . The expressions are [19]

$$\Delta S = \frac{1}{2\pi} \left[\frac{1}{6} \log\left(\frac{m_H^2}{m_{H^\pm}^2}\right) - \frac{5}{36} + \frac{m_H^2 m_A^2}{3(m_A^2 - m_H^2)^2} + \frac{m_A^4 (m_A^2 - 3m_H^2)}{6(m_A^2 - m_H^2)^3} \log\left(\frac{m_A^2}{m_H^2}\right) \right], \quad (15)$$

and

$$\Delta T = \frac{1}{32\pi^2 \alpha v^2} \left[F(m_{H^\pm}^2, m_A^2) + F(m_{H^\pm}^2, m_H^2) - F(m_A^2, m_H^2) \right] \quad (16)$$

where the function F is defined by

$$F(x, y) = \begin{cases} \frac{x+y}{2} - \frac{xy}{x-y} \log\left(\frac{x}{y}\right), & x \neq y, \\ 0, & x = y. \end{cases} \quad (17)$$

The T parameter vanishes when $m_{H^\pm} = m_H$ or $m_{H^\pm} = m_A$, since these conditions lead to an exact custodial $SU(2)$ symmetry, in which one of the neutral scalars joins the charged scalars to create a $SU(2)$ triplet. So to get proper oblique corrections, one knows that the key characters are the mass splittings of the Z_2 odd scalars, namely $\Delta M_1 \equiv m_H - m_{H^\pm}$ and $\Delta M_2 \equiv m_A - m_{H^\pm}$. In previous studies of scalar multiplets models, the mass splittings are limited by the previous S , T parameters fitted by the m_W mass of PDG. Now we have the right to reexamine the whole picture. In terms of ΔM_1 and ΔM_2 we could directly get the CDF W mass (the central value) by using Eq. 14, which is shown in Fig. 1 by the black dash-dotted line in ΔM_1 and ΔM_2 plane. We take $m_{H^\pm} = 300$ GeV as a benchmark model. In order to find the viable parameter regions, one should also consider the correlations to the W mass from the EW parameters. So we use the global EW best fit values of ΔS and ΔT derived in Ref. [7] (Table-III) to perform a fit by using $\chi^2(\mathbf{O}) = (\mathbf{y} - \mu(\mathbf{O}))^T \mathbf{C}^{-1} (\mathbf{y} - \mu(\mathbf{O}))$, where \mathbf{y} is the vector of central values and \mathbf{C} is the covariance matrix. In Fig. 1 we show 1- and 2-sigma regions allowed by ΔS and ΔT parameters in the mass splittings plane. The ΔT parameter becomes negative if the charged Higgs mass m_{H^\pm} falls into the range between the masses of the two neutral scalars, m_A and m_H . As a result, either $m_{H^\pm} > m_{A,H}$ or $m_{H^\pm} < m_{A,H}$ are permitted. Because of $S \sim \log(m_{H,A}/m_{H^\pm})$, the S parameter is disposed to be negative in the former scenario, which is disfavored by the global fit [7]. Then we only consider the case that charged Higgs is the lightest one in new higgs doublet.

The rich spectrum of the scalar sector also drives the evolution dynamics of the vacuum state non-trivial and provides the first order EWPT in the early Universe. By considering the thermal loop effects we use the approximated effective potential near the critical temperature [31]

$$V_{\text{eff}}(h, T) \approx \frac{1}{2}(-\mu^2 + cT^2)h^2 - \frac{\varepsilon T}{12\pi}(h^2)^{\frac{3}{2}} + \frac{\lambda}{4}h^4, \quad (18)$$

where the coefficient ε quantifies the interactions between the extra scalars and the Higgs boson. We have $\varepsilon \approx (6m_W^3 + 3m_Z^3)/v^3 + 2(\lambda_3/2)^{3/2} + ((\lambda_3 + \lambda_4 - \lambda_5)/2)^{3/2} + ((\lambda_3 + \lambda_4 + \lambda_5)/2)^{3/2}$ and $c \approx (6m_t^2 + 6m_W^2 + 3m_Z^2 + \frac{3}{2}m_H^2)/(12v^2) + (2\lambda_3 + \lambda_4)/12$.

The sizable oblique corrections favor large mass splittings ΔM_1 and ΔM_2 in order to interpret the new measured W boson mass, as shown in Fig. 1. So the quartic couplings λ_4, λ_5 in the effective potential directly link the new W deviation and the EWPT, then lead to an affected EWPT.

The symmetry breaking phase starts to nucleate right after the Universe cooling to the nucleation temperature T_n . The nucleation temperature is defined by the equality of the nucleation rate per Hubble volume and the Universe expansion rate, i.e. $\Gamma(T_n) = H^4(T_n)$, where $\Gamma(T) \sim T^4 e^{-S_3/T}$ is the decay rate per unit volume and S_3 is the classical action for the $O(3)$ symmetric bounce solution [32]. For a radiation-dominated Universe and a first order phase transition (FOPT) happening around the EW scale, T_n can be solved by $S_3/T_n \sim 140$ [33]. This criterion will be taken as the sufficient condition for a FOPT in this work. Further we use the package `cosmoTransition` [34] to calculate the bounce solution and T_n for the effective potential V_{eff} . The custodial symmetry in the scalar potential leads to a mass degeneration of m_A and m_{H^\pm} in previous research (or before the W mass deviation is identified). Generally, the EWPT strength depends on the mass splitting since it affects the potential barrier from custodial symmetry breaking. Now we have the chance to open the new parameter space by taking $m_A \neq m_{H^\pm}$, we can find that such mass splitting ΔM_2 enhances the EWPT strength in an obvious way, as shown in Fig. 1 with red-dashed contours. The reason is mainly that the larger ΔM_1 and/or ΔM_2 leads to a higher barrier between the symmetric vacuum and the symmetry breaking one. (see Eqs. 5, 6 and Eq. 18). This conclusion could also be generalized to other scalar multiplets

models.

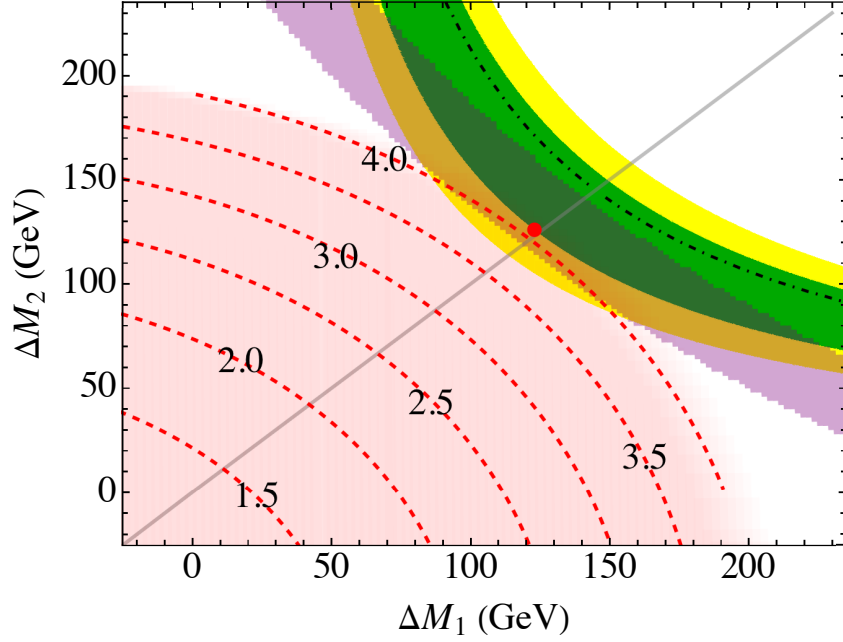


Figure 1: (Color online) Best fit region for $\Delta S, \Delta T$ operators, FOPT strength v_n/T_n and DM relic density, as functions of ΔM_1 and ΔM_2 where $\Delta M_1 \equiv m_H - m_{H^\pm}$ and $\Delta M_2 \equiv m_A - m_{H^\pm}$. The green and yellow bands correspond to the best fit with 1- and 2-sigma regions required by the new CDF measured m_W . The black dash-dotted line satisfies the central value of the CDF W mass. In the red region the strongly FOPT can be realized and the red dashed lines represent the contours of v_n/T_n . The gray line represents the condition $m_H = m_A$ which means that one cannot obtain the neutrino mass here. While the neutrino mass can be generated in the most parameter space with adjusted Yukawa couplings. In the purple region, one can yield the correct DM relic density $\Omega h^2 = 0.12 \pm 0.0012$ [28], with coupling $y_1 = 1.48 \times 10^{-12}$ and $m_{N_1} = 100$ GeV. The red point is the selected benchmark point (BP) to investigate GWs physics below, which is: $m_H = 423$ GeV, $m_A = 426$ GeV, $m_{H^\pm} = 300$ GeV, $\lambda_3 = 1.5$, $\lambda_4 = 2.98$, $\lambda_5 = -0.04$, $T_n = 158.78$ GeV, $v_n/T_n = 4.1$.

During a FOPT, stochastic GWs come from three sources: bubble collisions [35, 36], sound waves in the plasma [37, 38] and the magneto-hydrodynamics turbulence [39, 40]. Recent studies show that the bubble collision contribution to the GWs can generally be neglected because only a tiny fraction of the FOPT energy deposits in the bubble wall [41]. It turns out that the dominant contribution comes from the sound waves as most FOPT energy is pumped into the surrounding fluid shells [42]. Then the turbulence is another main source after a finite period of the sound wave [43]. Consequently, the GWs spectrum today can be expressed as (see details in supplementary file.)

$$\Omega_{\text{GW}}(f) = \Omega_{\text{sw}}(f) + \Omega_{\text{turb}}(f), \quad (19)$$

where f is the frequency, the subscripts “sw” and “turb” denote sound waves and turbulence respectively.

The GWs produced from a FOPT around EW scale have the potential to be probed by the next generation space-based laser interferometers such as LISA [44], BBO [45], TianQin [46, 47], Taiji [48–50], DECIGO [51, 52] and U-DECIGO [53]. In Fig. 2 we plot the GW spectrum with the benchmark point. We find that the GW signals are within the detectability of U-DECIGO, and this

possibility gives a complementary detection to the other searches. While to produce stronger signals one may consider the extension of the scalar sector, which further enhances the sensitivities [54].

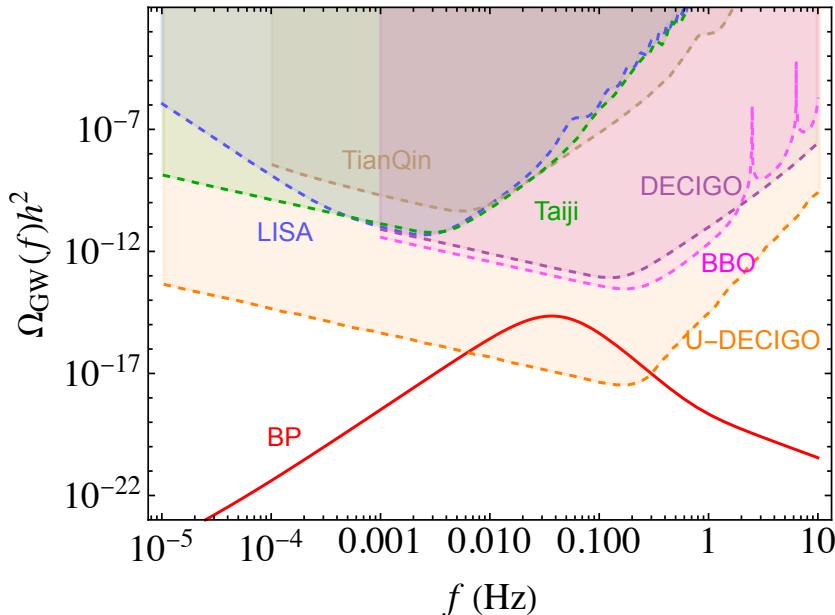


Figure 2: (Color online) GW spectrum $\Omega_{\text{GW}}h^2$ from the benchmark point where $\alpha = 0.021$, $\beta/H = 722.9$, depicted with the red line. The colored regions represent the expected sensitivities of the projected GWs interferometers.

4 Conclusion

Eventually, we successfully explain our Universe with the new measured W boson mass, the correct abundance of FIMP dark matter, and the Majorana neutrino masses within a minimal extension of the SM. We found that both neutrino mass and W boson mass are sensitive to the non-vanishing ΔM_1 and ΔM_2 , which also influences the freeze-in production of sterile neutrino dark matter. As a result, the non-degeneration between the charged and neutral components of a scotogenic scalar naturally links the three fundamental issues. More importantly, this model makes a precise prediction that will be validated in future GW experiments. The additional multiplet in the scalar sector drives the evolution dynamics of the vacuum state non-trivial. Thus in the early Universe, it provides a first-order electroweak phase transition, which is further enhanced by the new required mass splitting $m_A - m_{H^\pm}$. This is thought to be an efficient approach to generating detectable GWs. The future gravitational wave detectors will help reveal valuable information about the nature of this model.

Acknowledgements

This work was supported by the National Natural Science Foundation of China under the grants Nos. 11805161, 12005180, and 11975195, by the Natural Science Foundation of Shandong Province under Grant No. ZR2020QA083 and ZR2019JQ04 and by the Project of Shandong Province Higher Educational Science and Technology Program under Grants No. 2019KJJ007.

References

- [1] **CDF** Collaboration, T. Aaltonen et al., *High-precision measurement of the W boson mass with the CDF II detector*, *Science* **376** (2022), no. 6589 170–176.
- [2] J. de Blas, M. Ciuchini, E. Franco, A. Goncalves, S. Mishima, M. Pierini, L. Reina, and L. Silvestrini, *Global analysis of electroweak data in the Standard Model*, [[arXiv:2112.07274](#)].
- [3] **D0** Collaboration, V. M. Abazov et al., *Measurement of the W Boson Mass with the D0 Detector*, *Phys. Rev. Lett.* **108** (2012) 151804, [[arXiv:1203.0293](#)].
- [4] **ATLAS** Collaboration, M. Aaboud et al., *Measurement of the W -boson mass in pp collisions at $\sqrt{s} = 7$ TeV with the ATLAS detector*, *Eur. Phys. J. C* **78** (2018), no. 2 110, [[arXiv:1701.07240](#)]. [Erratum: *Eur.Phys.J.C* 78, 898 (2018)].
- [5] **LHCb** Collaboration, R. Aaij et al., *Measurement of the W boson mass*, *JHEP* **01** (2022) 036, [[arXiv:2109.01113](#)].
- [6] Y.-Z. Fan, T.-P. Tang, Y.-L. S. Tsai, and L. Wu, *Inert Higgs Dark Matter for New CDF W -boson Mass and Detection Prospects*, [[arXiv:2204.03693](#)].
- [7] C.-T. Lu, L. Wu, Y. Wu, and B. Zhu, *Electroweak Precision Fit and New Physics in light of W Boson Mass*, [[arXiv:2204.03796](#)].
- [8] P. Athron, A. Fowlie, C.-T. Lu, L. Wu, Y. Wu, and B. Zhu, *The W boson Mass and Muon $g - 2$: Hadronic Uncertainties or New Physics?*, [[arXiv:2204.03996](#)].
- [9] G.-W. Yuan, L. Zu, L. Feng, and Y.-F. Cai, *W -boson mass anomaly: probing the models of axion-like particle, dark photon and Chameleon dark energy*, [[arXiv:2204.04183](#)].
- [10] A. Strumia, *Interpreting electroweak precision data including the W -mass CDF anomaly*, [[arXiv:2204.04191](#)].
- [11] J. M. Yang and Y. Zhang, *Low energy SUSY confronted with new measurements of W -boson mass and muon $g-2$* , [[arXiv:2204.04202](#)].
- [12] J. de Blas, M. Pierini, L. Reina, and L. Silvestrini, *Impact of the recent measurements of the top-quark and W -boson masses on electroweak precision fits*, [[arXiv:2204.04204](#)].
- [13] C.-R. Zhu, M.-Y. Cui, Z.-Q. Xia, Z.-H. Yu, X. Huang, Q. Yuan, and Y. Z. Fan, *GeV antiproton/gamma-ray excesses and the W -boson mass anomaly: three faces of $\sim 60 - 70$ GeV dark matter particle?*, [[arXiv:2204.03767](#)].
- [14] A. Addazi, A. Marciano, A. P. Morais, R. Pasechnik, and H. Yang, *CDF II W -mass anomaly faces first-order electroweak phase transition*, [[arXiv:2204.10315](#)].
- [15] E. Ma, *Verifiable radiative seesaw mechanism of neutrino mass and dark matter*, *Phys. Rev. D* **73** (2006) 077301, [[hep-ph/0601225](#)].
- [16] S. Weinberg, *Baryon and Lepton Nonconserving Processes*, *Phys. Rev. Lett.* **43** (1979) 1566–1570.

- [17] N. G. Deshpande and E. Ma, *Pattern of Symmetry Breaking with Two Higgs Doublets*, *Phys. Rev. D* **18** (1978) 2574.
- [18] L. Lopez Honorez and C. E. Yaguna, *A new viable region of the inert doublet model*, *JCAP* **01** (2011) 002, [[arXiv:1011.1411](#)].
- [19] A. Arhrib, R. Benbrik, and N. Gaur, *$H \rightarrow \gamma\gamma$ in Inert Higgs Doublet Model*, *Phys. Rev. D* **85** (2012) 095021, [[arXiv:1201.2644](#)].
- [20] D. Borah and J. M. Cline, *Inert Doublet Dark Matter with Strong Electroweak Phase Transition*, *Phys. Rev. D* **86** (2012) 055001, [[arXiv:1204.4722](#)].
- [21] G. Gil, P. Chankowski, and M. Krawczyk, *Inert Dark Matter and Strong Electroweak Phase Transition*, *Phys. Lett. B* **717** (2012) 396–402, [[arXiv:1207.0084](#)].
- [22] Y. Li and C.-D. Lü, *Recent Anomalies in B Physics*, *Sci. Bull.* **63** (2018) 267–269, [[arXiv:1808.02990](#)].
- [23] N. Blinov, S. Profumo, and T. Stefaniak, *The Electroweak Phase Transition in the Inert Doublet Model*, *JCAP* **07** (2015) 028, [[arXiv:1504.05949](#)].
- [24] S. Fabian, F. Goertz, and Y. Jiang, *Dark matter and nature of electroweak phase transition with an inert doublet*, *JCAP* **09** (2021) 011, [[arXiv:2012.12847](#)].
- [25] E. Molinaro, C. E. Yaguna, and O. Zapata, *FIMP realization of the scotogenic model*, *JCAP* **07** (2014) 015, [[arXiv:1405.1259](#)].
- [26] A. G. Hessler, A. Ibarra, E. Molinaro, and S. Vogl, *Probing the scotogenic FIMP at the LHC*, *JHEP* **01** (2017) 100, [[arXiv:1611.09540](#)].
- [27] L. J. Hall, K. Jedamzik, J. March-Russell, and S. M. West, *Freeze-In Production of FIMP Dark Matter*, *JHEP* **03** (2010) 080, [[arXiv:0911.1120](#)].
- [28] **Planck** Collaboration, N. Aghanim et al., *Planck 2018 results. VI. Cosmological parameters*, *Astron. Astrophys.* **641** (2020) A6, [[arXiv:1807.06209](#)]. [Erratum: *Astron. Astrophys.* 652, C4 (2021)].
- [29] M. Abdughani, Y.-Z. Fan, L. Feng, Y.-L. S. Tsai, L. Wu, and Q. Yuan, *A common origin of muon $g-2$ anomaly, Galaxy Center GeV excess and AMS-02 anti-proton excess in the NMSSM*, *Sci. Bull.* **66** (2021) 2170–2174, [[arXiv:2104.03274](#)].
- [30] M. E. Peskin and T. Takeuchi, *Estimation of oblique electroweak corrections*, *Phys. Rev. D* **46** (1992) 381–409.
- [31] D. J. H. Chung, A. J. Long, and L.-T. Wang, *125 GeV Higgs boson and electroweak phase transition model classes*, *Phys. Rev. D* **87** (2013), no. 2 023509, [[arXiv:1209.1819](#)].
- [32] A. D. Linde, *Decay of the False Vacuum at Finite Temperature*, *Nucl. Phys. B* **216** (1983) 421. [Erratum: *Nucl. Phys. B* 223, 544 (1983)].
- [33] M. Quiros, *Finite temperature field theory and phase transitions*, pp. 187–259, 1, 1999. [hep-ph/9901312](#).

- [34] C. L. Wainwright, *CosmoTransitions: Computing Cosmological Phase Transition Temperatures and Bubble Profiles with Multiple Fields*, *Comput. Phys. Commun.* **183** (2012) 2006–2013, [[arXiv:1109.4189](#)].
- [35] S. J. Huber and T. Konstandin, *Gravitational Wave Production by Collisions: More Bubbles*, *JCAP* **09** (2008) 022, [[arXiv:0806.1828](#)].
- [36] Y. Di, J. Wang, R. Zhou, L. Bian, R.-G. Cai, and J. Liu, *Magnetic Field and Gravitational Waves from the First-Order Phase Transition*, *Phys. Rev. Lett.* **126** (2021), no. 25 251102, [[arXiv:2012.15625](#)].
- [37] M. Hindmarsh, S. J. Huber, K. Rummukainen, and D. J. Weir, *Numerical simulations of acoustically generated gravitational waves at a first order phase transition*, *Phys. Rev. D* **92** (2015), no. 12 123009, [[arXiv:1504.03291](#)].
- [38] H.-K. Guo, K. Sinha, D. Vagie, and G. White, *Phase Transitions in an Expanding Universe: Stochastic Gravitational Waves in Standard and Non-Standard Histories*, *JCAP* **01** (2021) 001, [[arXiv:2007.08537](#)].
- [39] P. Binetruy, A. Bohe, C. Caprini, and J.-F. Dufaux, *Cosmological Backgrounds of Gravitational Waves and eLISA/NGO: Phase Transitions, Cosmic Strings and Other Sources*, *JCAP* **06** (2012) 027, [[arXiv:1201.0983](#)].
- [40] C. Caprini, R. Durrer, and G. Servant, *The stochastic gravitational wave background from turbulence and magnetic fields generated by a first-order phase transition*, *JCAP* **12** (2009) 024, [[arXiv:0909.0622](#)].
- [41] D. Bodeker and G. D. Moore, *Electroweak Bubble Wall Speed Limit*, *JCAP* **05** (2017) 025, [[arXiv:1703.08215](#)].
- [42] J. Ellis, M. Lewicki, and J. M. No, *On the Maximal Strength of a First-Order Electroweak Phase Transition and its Gravitational Wave Signal*, *JCAP* **04** (2019) 003, [[arXiv:1809.08242](#)].
- [43] J. Ellis, M. Lewicki, and J. M. No, *Gravitational waves from first-order cosmological phase transitions: lifetime of the sound wave source*, *JCAP* **07** (2020) 050, [[arXiv:2003.07360](#)].
- [44] **LISA** Collaboration, P. Amaro-Seoane et al., *Laser Interferometer Space Antenna*, [[arXiv:1702.00786](#)].
- [45] J. Crowder and N. J. Cornish, *Beyond LISA: Exploring future gravitational wave missions*, *Phys. Rev. D* **72** (2005) 083005, [[gr-qc/0506015](#)].
- [46] **TianQin** Collaboration, J. Luo et al., *TianQin: a space-borne gravitational wave detector*, *Class. Quant. Grav.* **33** (2016), no. 3 035010, [[arXiv:1512.02076](#)].
- [47] Y.-M. Hu, J. Mei, and J. Luo, *Science prospects for space-borne gravitational-wave missions*, *Natl. Sci. Rev.* **4** (2017), no. 5 683–684.
- [48] W.-R. Hu and Y.-L. Wu, *The Taiji Program in Space for gravitational wave physics and the nature of gravity*, *Natl. Sci. Rev.* **4** (2017), no. 5 685–686.

- [49] W.-H. Ruan, Z.-K. Guo, R.-G. Cai, and Y.-Z. Zhang, *Taiji program: Gravitational-wave sources*, *Int. J. Mod. Phys. A* **35** (2020), no. 17 2050075, [[arXiv:1807.09495](#)].
- [50] Z.-W. Zhao, L.-F. Wang, J.-F. Zhang, and X. Zhang, *Prospects for improving cosmological parameter estimation with gravitational-wave standard sirens from Taiji*, *Sci. Bull.* **65** (2020), no. 16 1340–1348, [[arXiv:1912.11629](#)].
- [51] S. Kawamura et al., *The Japanese space gravitational wave antenna: DECIGO*, *Class. Quant. Grav.* **28** (2011) 094011.
- [52] S. Kawamura et al., *The Japanese space gravitational wave antenna DECIGO*, *Class. Quant. Grav.* **23** (2006) S125–S132.
- [53] H. Kudoh, A. Taruya, T. Hiramatsu, and Y. Himemoto, *Detecting a gravitational-wave background with next-generation space interferometers*, *Phys. Rev. D* **73** (2006) 064006, [[gr-qc/0511145](#)].
- [54] L. Bian and X. Liu, *Two-step strongly first-order electroweak phase transition modified FIMP dark matter, gravitational wave signals, and the neutrino mass*, *Phys. Rev. D* **99** (2019), no. 5 055003, [[arXiv:1811.03279](#)].